

Received July 4, 2017, accepted July 25, 2017, date of publication August 1, 2017, date of current version August 22, 2017.

Digital Object Identifier 10.1109/ACCESS.2017.2734739

# Performance Analysis for SDMA mmWave Systems: Using an Approximate Closed-Form Solution of Downlink Sum-Rate

LIN BAI<sup>1</sup>, (Senior Member, IEEE), TIAN LI<sup>1,2</sup>, (Student Member, IEEE),  
ZHENYU XIAO<sup>1,2</sup>, (Senior Member, IEEE), AND JINHO CHOI<sup>3</sup>, (Senior Member, IEEE)

<sup>1</sup>School of Electronic and Information Engineering, Beihang University, Beijing 100191, China

<sup>2</sup>Beijing Laboratory for General Aviation Technology, Beihang University, Beijing 100191, China

<sup>3</sup>School of Electrical Engineering and Computer Science, Gwangju Institute of Science and Technology, Gwangju 61005, South Korea

Corresponding author: Zhenyu Xiao (xiaozy@buaa.edu.cn)

This work was supported by the National Natural Science Foundation of China under Grant 61571025, Grant 61231011, and Grant 61231013.

**ABSTRACT** In this paper, we analyze the performance of downlink transmission in a space division multiple access (SDMA) millimeter-wave (mmWave) system with beam selection, where antenna arrays are considered at a base station (BS) and users. Under the assumption of limited scattering environment, we propose a simplified approach to analyze the downlink performance of the SDMA system. In this scheme, the throughput for each BS beam is approximated by a binary random variable for tractable analysis and an approximate closed-form solution for the downlink sum rate is derived. It is shown that the predicted throughputs by the proposed method reasonably agree with simulation results.

**INDEX TERMS** Space division multiple access (SDMA), millimeter wave (mmWave), antenna arrays, performance analysis, binary random variable.

## I. INTRODUCTION

The millimeter-wave (mmWave) band, which can provide a large available spectral resources [1]–[4], has been widely studied for the next generation cellular system, namely 5G, to meet the high-speed wireless service requirements [5]. Compared with ultra high frequency (UHF) bands employed in existing cellular systems, signals transmitted over an mmWave channel may experience high path loss [6]–[8]. Thus, it is generally expected to have few paths in mmWave band [1], [9]–[11]. The resulting environment is referred to as limited scattering environment as opposed to rich scattering environment that is typical in UHF bands.

In space division multiple access (SDMA) systems, different downlink transmission strategies have been studied in UHF bands [12]–[14], where beamforming at a base station (BS) plays a significant role in compensating for the high propagation attenuation and improving spectral efficiency [15]–[20]. For beamforming in mmWave systems, antenna arrays with a large number of elements are generally equipped at the BS and users to extend communication range [1], [21]. Unfortunately, due to the large-scale antenna arrays, the implementation of radio frequency (RF) hardware has become one of the main difficulties in mmWave

systems [22]. In such a case, hybrid beamforming using analog and digital beamformers has been studied to solve this implementation constraint [23], [24]. With a small number of RF chains, [11] proposed a hybrid precoder using analog phase shifters and digital precoders under limited scattering environments. In [25], Rajashekar and Hanzo considers a hybrid beamformer for a more practical system, where the hybrid beamforming matrices are designed by employing a finite input alphabet instead of Gaussian symbols. As an alternative approach, beam selection with a set of pre-determined beams can also be considered [26]. One of the advantages of beam selection lies in the low-complexity of beamforming compared with conventional hybrid approaches. Specifically, beam selection in mmWave systems is a special case of hybrid beamforming, in which the digital beamformer can be seen as an analog beam selector.

The above mentioned works mainly consider beamforming methods for mmWave systems, where performance was valued by simulation. To the best of our knowledge, few studies have been focused on the performance analysis of mmWave systems with beamforming, especially on deriving closed-form expression of achievable sum-rate. Different from these works, in this paper we analyze the performance

of downlink SDMA in an mmWave system with beam selection [12]. The performance analysis is challenging due to the interaction between user beamforming [27], [28] and BS beamforming with pre-determined codebooks for beam selection. Therefore, with certain assumptions for tractable analysis, we propose approximate closed-form solutions for the downlink sum-rate under different channel conditions, where the throughput of each BS beam is approximated by a binary random variable. With these manipulations, we derive an approximate closed-form expression for downlink throughput in SDMA mmWave systems. Numerical results show that the analytical sum-rate performance derived by the proposed method reasonably agree with simulation results.

The rest of the paper is organized as follows. Section II presents the system model for SDMA mmWave systems using antenna arrays and discusses the downlink sum-rate with user beam selection strategy. Furthermore, some necessary assumptions for tractable analysis are also studied. In order to apply the simplified approach to analyze the performance, the effectiveness of user beamforming is discussed in Section III. In Section IV, approximate closed-form solutions for downlink throughput with different channel coefficient conditions are derived and the effect of the number of BS beams on downlink performance is analyzed. Simulation results are presented and discussed in Section V and the paper is concluded in Section VI.

*Notation:* Vectors and matrices are presented by lowercase and uppercase bold letters, respectively. The transpose and Hermitian transpose are denoted by superscripts T and H, respectively. Present by  $\mathbb{C}^{n \times m}$  as the  $n \times m$ -dimensional complex space. The statistical expectation is presented by  $\mathbb{E}[\cdot]$ . While  $\mathcal{CN}(\mathbf{a}, \mathbf{R})$  denotes the distribution of circularly symmetric complex Gaussian (CSCG) random vectors with mean vector  $\mathbf{a}$  and covariance matrix  $\mathbf{R}$ .

## II. ANALYSIS OF USER BEAM SELECTION IN mmWave SYSTEMS

In this section, we consider an opportunistic SDMA with user beam selection based on [12].

### A. SYSTEM MODEL

Throughout the paper, we consider a frequency-division duplexing (FDD) based cellular system constitutes one BS and  $U$  users. As shown in Fig. 1, antenna arrays with  $L_B$  and  $L_U$  elements are equipped at the BS and users, respectively. Although hybrid beamforming implementation is employed in mmWave systems, the computational complexity is still high as full channel state information (CSI) feedback and precoding are required. Thus, in this paper, we assume that the beams are formed by analog beamformers with pre-determined phases (i.e., a hybrid beamformer where the beamforming is implemented in RF domain and the digital precoding is merely a beam selector) at the BS. In this case, beamforming becomes beam selection with a set of pre-determined beams.

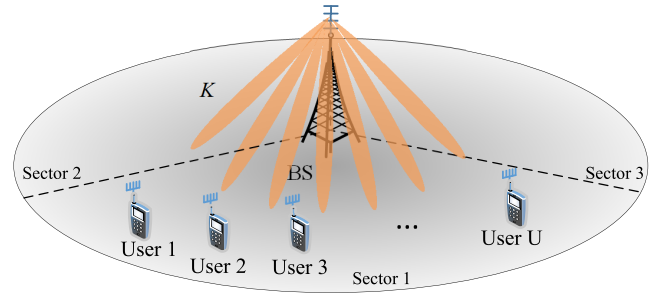


FIGURE 1. System model for the SDMA mmWave system with beam selection.

Let  $\mathcal{V}$  be the set of beams at the BS and  $|\mathcal{V}| = K$ . The downlink pilot signal from the BS array is given by

$$\mathbf{z} = \sum_{k=1}^K \mathbf{v}_k d_k \quad (1)$$

where  $\mathbf{v}_k$  is the  $k$ -th beam in  $\mathcal{V}$  and  $d_k$  is the pilot signal for the  $k$ -th beam. Hence, the received signal vector at user  $u$  becomes

$$\begin{aligned} \mathbf{y}_u &= \mathbf{H}_u \mathbf{z} + \mathbf{n}_u \\ &= \sum_{k=1}^K \mathbf{H}_u \mathbf{v}_k d_k + \mathbf{n}_u \end{aligned} \quad (2)$$

where  $\mathbf{H}_u \in \mathbb{C}^{L_U \times L_B}$  denotes the downlink channel to user  $u$ , and  $\mathbf{n}_u \sim \mathcal{CN}(\mathbf{0}, \sigma^2 \mathbf{I})$  denotes the background noise vector. Moreover, we assume  $\mathbb{E}[|d_k|^2] = P/K$ , i.e., the total transmit power is  $P$ .

According to [9] and [29], mmWave channels would be characterized by few strong paths. Thus, the channel matrix,  $\mathbf{H}_u$ , can be found as

$$\mathbf{H}_u = \sum_{p=1}^Q h_{u,p} \mathbf{b}(\psi_{u,p}) \mathbf{a}^H(\theta_{u,p}) \quad (3)$$

where  $Q$  is the number of paths between the BS and a user. For simplicity, we assume that the number of paths is the same for all users. As mentioned above, due to limited scattering in mmWave channels,  $Q$  is not large and usually 2 or 3 on average [9]. Let  $h_{u,p}$  denote the channel coefficient of the  $p$ -th path. The angle-of-arrival (AoA) and angle-of-departure (AoD) are presented by  $\psi_{u,p}$  and  $\theta_{u,p}$ , respectively. In this paper, we assume that  $\psi_{u,p}$  and  $\theta_{u,p}$  are independent and uniformly distributed. Here,  $\mathbf{b}(\psi) \in \mathbb{C}^{L_U \times 1}$  and  $\mathbf{a}(\theta) \in \mathbb{C}^{L_B \times 1}$  denote the array response vectors (ARVs) of the user and BS arrays, respectively. For the sake of simplicity, we consider a uniform linear array (ULA) with half-wavelength spacing and the ARVs are normalized as  $\|\mathbf{b}(\psi)\| = \|\mathbf{a}(\theta)\| = 1$ . In this case, the ARV of the BS becomes

$$\mathbf{a}(\theta) = \frac{1}{\sqrt{L_B}} [1 e^{-j\pi \sin \theta} \dots e^{-j(L_B-1)\pi \sin \theta}]^T. \quad (4)$$

Although the ULA is considered in the paper, it is straightforward to extend the channel model and beam selection with uniform planar array (UPA) [11], because similar assumptions as **S1**- **S2**) in Subsection II-C could also be satisfied to simplify the analysis.

It is noteworthy that multiple mini-slots of random orthogonal beams are used in [12] for beam selection under a rich scattering environment. To find the best set of random orthogonal beams for a given group of users, multiple sets of beams are generated and transmitted over multiple mini-slots. Thus, it is desirable to have more sets of random orthogonal beams or more mini-slots for a better performance. However, since the pilot signaling overhead increases with the number of mini-slots, there is a trade-off and an optimal number of mini-slots can be found [12]. In mmWave channels, as mentioned earlier, due to limited scattering environments, multiple sets of beams may not be useful to understand the system performance which has been studied in [30]. In this paper, with a set of  $K$  near orthogonal beams that are obtained by the ARV of the BS with quantized AoDs, the pilot training can be carried out as above. Note that in our case, we do not use multiple mini-slots (we only use one slot).

### B. USER BEAM SELECTION AND DOWNLINK THROUGHPUT

Due to the implementation difficulties and computational complexity, in this paper, we consider analog beamformer with fixed-beams at users.

Suppose that each user has a codebook of pre-determined beamforming vectors, which is denoted by  $\mathcal{W}_u = \{\mathbf{w}_{u,1}, \dots, \mathbf{w}_{u,N_U}\}$ , where  $N_U$  represents the number of beams at a user. From (2), the beamformer output of the  $q$ -th beam at user  $u$  becomes

$$s_{u,q;k} = \mathbf{w}_{u,q}^H \mathbf{y}_u = \mathbf{w}_{u,q}^H \mathbf{H}_u \mathbf{v}_k d_k + \sum_{l \neq k} \mathbf{w}_{u,q}^H \mathbf{H}_u \mathbf{v}_l d_l + \mathbf{w}_{u,q}^H \mathbf{n}_u. \quad (5)$$

Throughout the paper, we assume  $\|\mathbf{v}_k\| = \|\mathbf{w}_{u,q}\| = 1$  for normalization purposes.

At user  $u$ , from (5), the signal-to-interference-plus-noise ratio (SINR) of BS beam  $k$  at user beam  $q$  can be written as

$$A_{u,q;k} = \frac{|\mathbf{w}_{u,q}^H \mathbf{H}_u \mathbf{v}_k|^2}{K/\rho + \sum_{l \neq k} |\mathbf{w}_{u,q}^H \mathbf{H}_u \mathbf{v}_l|^2} \quad (6)$$

where  $\rho = P/\sigma^2$ . In (6), the interference power term,  $\sum_{l \neq k} |\mathbf{w}_{u,q}^H \mathbf{H}_u \mathbf{v}_l|^2$ , is regarded as the inter-beam interference (IBI) results from the other beams. Thus, the SINR related to the  $k$ -th BS beam at user  $u$  is given by

$$A_{u;k} = \max_{1 \leq q \leq N_U} A_{u,q;k}. \quad (7)$$

According to [12], based on the users' feedback signals (BS beam indexes and the corresponding SINR values), the BS allocates the  $k$ -th beam to the user with the highest SINR.

Then, the downlink throughput can be computed as

$$C = \sum_{k=1}^K \log_2 \left( 1 + \max_{1 \leq u \leq U} A_{u;k} \right). \quad (8)$$

While the beam selection approach is based on [12], its performance analysis is different from that in [12] due to various reasons. One of them is the existence of user arrays. Another is the different channel environment. In the following analysis, we consider the beam selection under limited scattering environments.

### C. SIMPLIFICATIONS USING mmWave CHARACTERS

For tractable reasons, we have the following assumptions according to the characters of mmWave.

**S1)** Denote  $\Psi_q$  as the set of possible AoAs of the received signals related to the  $q$ -th user beam. Let  $\cup_q \Psi_q = \Psi$ , and we assume that

$$|\mathbf{w}_{u,q}^H \mathbf{b}(\psi)|^2 = \begin{cases} 1, & \text{if } \psi \in \Psi_q; \\ \epsilon_U, & \text{otherwise} \end{cases} \quad (9)$$

where  $\epsilon_U \ll 1$  and  $\Psi_j \cap \Psi_q = \emptyset, j \neq q$ . Moreover,  $\Psi_q$ 's are equally divided and  $q = 1, \dots, N_U$ .

As discussed in **S1**), the entire space of the AoAs can be covered by user beams,  $\{\mathbf{w}_{u,1}, \dots, \mathbf{w}_{u,N_U}\}$ , shown in Fig. 2. Clearly, if  $\psi \notin \Psi_q$ , we have  $|\mathbf{w}_{u,q}^H \mathbf{b}(\psi)|^2 = \epsilon_U \ll 1$ . Note that  $\mathbf{w}_{u,q}$  would be the ARV of the center AoA of  $\Psi_q$ . In this case, for  $\psi \in \Psi_q$ , the claim that  $|\mathbf{w}_{u,q}^H \mathbf{b}(\psi)|^2 = 1$  in **S1**) may not be true, but the approximation would be reasonable since  $L_U$  is expected to be large in mmWave systems.

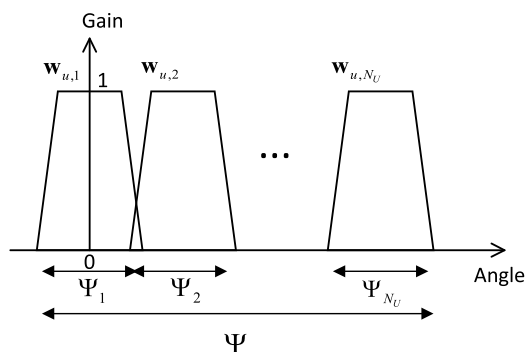


FIGURE 2. An illustration of the set of user beams.

**S2)** The beamforming vectors at the BS are generated as

$$|\mathbf{a}^H(\theta) \mathbf{v}_k|^2 = \begin{cases} 1, & \text{if } \theta \in \Theta_k; \\ \epsilon_B, & \text{otherwise} \end{cases} \quad (10)$$

where  $\Theta_k$  denotes the set of the AoDs for the  $k$ -th BS beam. Again,  $\Theta_k$ 's are equally divided. Furthermore,  $\Theta_k \cap \Theta_m = \emptyset, k \neq m$ , and  $\cup_k \Theta_k = \Theta$ , where  $\Theta$  is the set of all possible AoDs.

The rationale of **S2**) is similar to that of **S1**) and is omitted here.

### III. THE EFFECT OF USER BEAMFORMING

In this section, based on the discussions in Subsection II-C, we focus on the role of the user beamformer with the channel matrix described in (3) and propose a simplified model for user beamforming.

Under **S1** - **S2**), we have the following definition.

*Definition 1:* With  $Q$  paths, suppose that

$$\theta_{u,1} \in \Theta_1, \quad \theta_{u,2} \in \Theta_2, \dots, \theta_{u,Q} \in \Theta_Q. \quad (11)$$

It is claimed that user beamforming is *effective* if

$$|\mathbf{w}_{u,i}^H \mathbf{b}(\psi_{u,j})|^2 = \begin{cases} 1, & i = j; \\ \epsilon_U, & i \neq j, \end{cases}$$

for  $i = 1, \dots, N_U$  and  $j = 1, \dots, Q$ . (12)

Otherwise, it is *ineffective*.

For illustration purpose, the case of *ineffective* beamforming with  $Q = 2$  is shown in Fig. 3, where  $\theta_{u,1} \in \Theta_1$  and  $\theta_{u,2} \in \Theta_2$ . We can find that  $|\mathbf{w}_{u,j}^H \mathbf{b}(\psi_{u,1})|^2 = |\mathbf{w}_{u,j}^H \mathbf{b}(\psi_{u,2})|^2 = 1$  based on **S1**). Thus, the spatial diversity at the user side cannot be fully exploited which results in *ineffective* user beamforming.

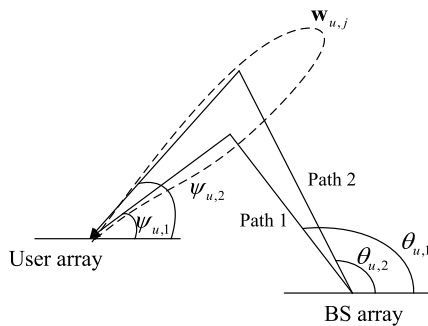


FIGURE 3. An illustration of ineffective beamforming with  $Q = 2$ .

Denote by  $P_e(Q)$  the probability of *effective* user beamforming with  $Q$  paths. Then, we have the following results.

*Lemma 1:* Under **S1** - **S2**), we assume that  $\theta_{u,i}$ , for  $i = 1, \dots, Q$ , where  $Q < K$ , is in a different  $\Theta_l$ ,  $l = 1, \dots, K$ . For any  $Q \geq 2$ ,  $P_e(Q)$  becomes

$$P_e(Q) = \frac{\prod_{i=1}^{Q-1} (N_U - i)}{N_U^{Q-1}}. \quad (13)$$

*Proof:* As we assume that  $Q$  paths are located in different BS beams (suppose that  $Q = 2$ , if  $\theta_{u,1} \in \Psi_1$  and  $\theta_{u,2} \in \Psi_1$ , the two paths are merged, this becomes the case of  $Q = 1$ ). Let  $\psi_{u,1} \in \Psi_1$ , we have  $\Pr(\psi_{u,2} \notin \Psi_1) = \frac{N_U - 1}{N_U}$ . If  $\psi_{u,2} \in \Psi_2$ , we have  $\Pr(\psi_{u,3} \notin \Psi_1 \cup \Psi_2) = \frac{N_U - 2}{N_U}$ . Thus, the probability of (12) becomes  $\frac{\prod_{i=1}^{Q-1} (N_U - i)}{N_U^{Q-1}}$ . ■

As a result, the probability of *effective* user beamforming decreases with  $Q$  for a large  $N_U$ . To illustrate it intuitively, the probabilities of *effective* user beamforming with different values of  $Q$  are shown in Fig. 4, where  $K = 20$  and  $N_U = \{40, 50\}$ .

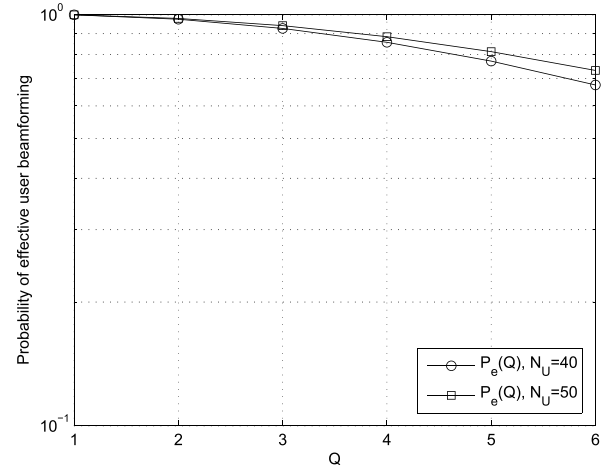


FIGURE 4. The probability of effective user beamforming with  $Q$ .

Clearly, we can find that the probability of the *effective* beamforming decreases with  $Q$  which confirms (13). Moreover, it is noteworthy that the value of the probability is prohibitively high under limited scattering environment and  $P_e(Q) = 0.9263$  with  $Q = 3$  when  $N_U = 40$ . That is, with a high probability, there might be a user beam  $q$  that satisfies  $|\mathbf{w}_{u,q}^H \mathbf{b}(\psi_{u,p})|^2 = 1$  for a  $p$  of  $|\mathbf{a}^H(\theta_{u,p}) \mathbf{v}_k|^2 = 1$ . This is regarded as *effective* user beamforming. With the approximation of *effective* user beamforming, we can simplify the performance analysis of downlink transmission in mmWave systems.

### IV. PERFORMANCE ANALYSIS OF DOWNLINK SDMA mmWave SYSTEMS

In this section, we discuss the downlink throughput for the performance analysis. According to (13), we assume that the user beamforming is *effective*. In this case, with certain characters of mmWave, we model the channel coefficient as a constant value and derive an approximate downlink throughput by using a binary random model of the SINRs. After that, we consider the impact of the number of BS beams on the downlink throughput. Moreover, to validate the performance trend over  $K$ , we also analyze the system performance with Rayleigh fading channel coefficients and provide a closed-form expression of the achievable sum-rate.

#### A. AN APPROXIMATE CLOSED-FORM SOLUTION FOR DOWNLINK SUM-RATE

To derive the approximate closed-form expression of the system achievable throughput, we first consider the following assumption.

**S3)** The channel gains are the same for all  $u$  and  $p$  [29], i.e.,

$$|h_{u,p}|^2 = |h|^2 = 1. \quad (14)$$

In **S3**), considering the independent path loss of different paths, the channel coefficient in (14) is not generally true. However, with this assumption, we can analyze the impact

of  $K$  on system performance intuitively. Moreover, when the distances between the BS and users are almost the same, such as air-based network communications, it would be reasonable to set the channel coefficient as a constant.

*Lemma 2:* Under **S1** - **S3**,  $A_{u;k}$  can be formulated as a random variable given by

$$A_{u;k} \begin{cases} \geq \mu & \text{w.p. } P_\mu; \\ \leq \lambda & \text{w.p. } 1 - P_\mu \end{cases} \quad (15)$$

where  $\mu = \frac{1}{K/\rho + (K-1)\epsilon_B}$ ,  $\lambda = \frac{1}{K-1}$ , and  $P_\mu = 1 - e^{-\frac{Q}{K}}$ .

*Proof:* Suppose that there exists at least one path  $p$  such that  $|\mathbf{a}^H(\theta_{u,p})\mathbf{v}_k|^2 = 1$  for a user. The resulting SINR in (7) is given by

$$\begin{aligned} A_{u;k} &= \max_q \frac{|\mathbf{w}_{u,q}^H \sum_{p=1}^Q h_{u,p} \mathbf{b}(\psi_{u,p}) \mathbf{a}^H(\theta_{u,p}) \mathbf{v}_k|^2}{K/\rho + \sum_{l \neq k} |\mathbf{w}_{u,q}^H \sum_{p=1}^Q h_{u,p} \mathbf{b}(\psi_{u,p}) \mathbf{a}^H(\theta_{u,p}) \mathbf{v}_l|^2} \\ &= \frac{|\sum_{p=1}^Q h_{u,p} \mathbf{a}^H(\theta_{u,p}) \mathbf{v}_k|^2}{K/\rho + \sum_{l \neq k} |\sum_{p=1}^Q h_{u,p} \mathbf{a}^H(\theta_{u,p}) \mathbf{v}_l|^2} \\ &\geq \max_p \frac{|\mathbf{a}^H(\theta_{u,p}) \mathbf{v}_k|^2}{K/\rho + \sum_{l \neq k} |\mathbf{a}^H(\theta_{u,p}) \mathbf{v}_l|^2}, \end{aligned} \quad (16)$$

because there is a user beam, say user beam  $q$ , that satisfies  $|\mathbf{w}_{u,q}^H \mathbf{b}(\psi_{u,p})|^2 = 1$  for a  $p$  of  $|\mathbf{a}^H(\theta_{u,p}) \mathbf{v}_k|^2 = 1$ . Due to **S2**, we have

$$A_{u;k} \geq \mu = \frac{1}{K/\rho + (K-1)\epsilon_B}. \quad (17)$$

The probability of (17) is equivalent to the probability that there is at least one path that belongs to the  $k$ -th beam, which can be calculated as

$$\begin{aligned} P_\mu &= 1 - \Pr(|\mathbf{a}^H(\theta_{u,p}) \mathbf{v}_k|^2 \leq \epsilon_B \text{ for all } p) \\ &= 1 - \left(\frac{K-1}{K}\right)^Q. \end{aligned} \quad (18)$$

Since  $\frac{K-1}{K}$  can be written as  $2^{\log_2(1-\frac{1}{K})}$  and  $\log_2(1+x) \approx x \log_2 e$  when  $x \approx 0$ , (18) becomes

$$\begin{aligned} P_\mu &= 1 - \left(2^{\log_2(1-\frac{1}{K})}\right)^Q \\ &\approx 1 - \left(2^{-\frac{1}{K} \log_2 e}\right)^Q \\ &= 1 - e^{-\frac{Q}{K}} \end{aligned} \quad (19)$$

where the inequality tends to equality increasingly with  $K$ .

On the other hand, if the  $k$ -th BS beam is not included in all paths of a user, the SINR becomes either  $A_{u;k} = \frac{\epsilon_B}{K/\rho + (K-1)\epsilon_B}$  or  $\frac{\epsilon_B}{K/\rho + 1 + (K-2)\epsilon_B}$  (i.e., one of  $|\mathbf{a}^H(\theta_{u,p}) \mathbf{v}_l|^2$ ,  $l \neq k$  is 1), which satisfies

$$A_{u;k} \leq \lambda = \frac{1}{K-1}. \quad (20)$$

The corresponding probability is  $1 - P_\mu$ .  $\blacksquare$

According to Lemma 2, for tractable analysis,  $A_{u;k}$  would be modeled as a binary random variable with  $A_{u;k} \in \{\mu, \lambda\}$  and the  $A_{u;k}$ 's are independent. Thus, the throughput for each BS beam,  $X_k$ , becomes a binomial random variable given by

$$\begin{aligned} X_k &= \max_{1 \leq u \leq U} \log_2(1 + A_{u;k}) \\ &= \begin{cases} \log_2(1 + \mu), & \text{w.p. } P_\mu(U); \\ \log_2(1 + \lambda), & \text{w.p. } 1 - P_\mu(U) \end{cases} \end{aligned} \quad (21)$$

where

$$\begin{aligned} P_\mu(U) &= 1 - (1 - P_\mu)^U \\ &\approx 1 - e^{-\frac{QU}{K}}. \end{aligned} \quad (22)$$

From (8), since  $C = \sum_{k=1}^K X_k$ , the mean of  $C$  can be calculated as

$$\begin{aligned} \mathbb{E}[C] &= \sum_{k=1}^K \mathbb{E}[X_k] \\ &= K \left[ \log_2(1 + \mu) P_\mu(U) + \log_2(1 + \lambda) (1 - P_\mu(U)) \right] \\ &\approx K \log_2 \left( 1 + \frac{1}{K/\rho + (K-1)\epsilon_B} \right) (1 - e^{-\frac{QU}{K}}). \end{aligned} \quad (23)$$

Note that the approximation is reasonable since  $\log_2(1 + \lambda)$  can be ignored with a sufficiently large  $K$ .

## B. THROUGHPUT ANALYSIS

In UHF band, under a rich scattering environment, the downlink throughput can be optimized by adjusting the number of training mini-slots in [12]. As mentioned earlier, in mmWave band, due to limited scattering environments, we do not need to have multiple mini-slots of random orthogonal beams. There is a single slot of  $K$  beams. To see the impact of the number of beams,  $K$ , on the average throughput in (23), we consider the case that  $K \leq U$ . It follows

$$\begin{aligned} \mathbb{E}[C] &= K \log_2 \left( 1 + \frac{1}{K/\rho + (K-1)\epsilon_B} \right) (1 - e^{-\frac{QU}{K}}) \\ &\approx K \log_2 \left( 1 + \frac{1}{K/\rho + (K-1)\epsilon_B} \right) \\ &\approx K \log_2 \left( 1 + \frac{1}{\xi K} \right) \end{aligned} \quad (24)$$

where  $\xi = \frac{1}{\rho} + \epsilon_B$  that can be considered as a constant since  $\epsilon_B \ll 1$  with near orthogonal beams. Let  $\bar{R}(K) = K \log_2 \left( 1 + \frac{1}{\xi K} \right)$ . The derivative of the average throughput with respect to  $K$  becomes

$$\begin{aligned} \frac{d}{dK} \bar{R}(K) &= \frac{1}{\ln 2} \left( \ln \left( 1 + \frac{1}{\xi K} \right) - \frac{1}{1 + \xi K} \right) \\ &\geq \frac{1}{\ln 2} \left( \frac{1}{1 + \xi K} - \frac{1}{1 + \xi K} \right) \\ &= 0 \end{aligned} \quad (25)$$

where the inequality is due to  $\ln(1+x) \geq \frac{x}{1+x}$  for  $x \geq 0$ . Thus,  $\bar{R}(K)$  is a nondecreasing function of  $K$ . That is, the

more near orthogonal BS beams generated simultaneously (i.e., more angular resolution), the higher the sum throughput in downlink SDMA mmWave systems. However, the limit of  $\bar{R}(K)$  is bounded as

$$\begin{aligned} \lim_{K \rightarrow \infty} \bar{R}(K) &= \frac{\log_2 e}{\xi} \\ &= \log_2 e \frac{\rho}{1 + \rho \epsilon_B}. \end{aligned} \quad (26)$$

It is noteworthy that when  $\rho \rightarrow \infty$ , the performance would be limited by  $\epsilon_B$ . That is, if  $\rho \rightarrow \infty$ , the asymptotic sum-rate approaches  $\frac{\log_2 e}{\epsilon_B}$ . Thus, a small  $\epsilon_B$  is generally desirable.

### C. PERFORMANCE ANALYSIS UNDER RAYLEIGH FADING CHANNELS

Without loss of generality, in this subsection, we discuss the system performance with small-scale fading channel coefficient. As in [11], the channel coefficients,  $h_{u,p}$ 's, are assumed to be i.i.d.  $\mathcal{CN}(0, 1)$  here. For convenience, we use  $h$  instead of  $h_{u,p}$  in the following analysis. Then,  $X_k$  in (21) becomes

$$X_k = \begin{cases} \log_2 \left( 1 + \frac{|h|^2}{K/\rho + (K-1)\epsilon_B|h|^2} \right), & \text{w.p. } P_\mu(U); \\ \log_2 \left( 1 + \frac{1}{K-1} \right), & \text{w.p. } 1 - P_\mu(U), \end{cases} \quad (27)$$

and the average sum-rate is derived as

$$\begin{aligned} \mathbb{E}[C] &= \sum_{k=1}^K \mathbb{E}[X_k] \\ &= K \mathbb{E} \left[ \log_2 \left( 1 + \frac{|h|^2}{K/\rho + (K-1)\epsilon_B|h|^2} \right) \right] P_\mu(U) \\ &\quad + K \log_2 \left( 1 + \frac{1}{K-1} \right) (1 - P_\mu(U)) \\ &\approx K \mathbb{E} \left[ \log_2 \left( 1 + \frac{|h|^2}{K/\rho + (K-1)\epsilon_B|h|^2} \right) \right] P_\mu(U) \\ &= K \int_0^\infty \log_2 \left( 1 + \frac{x}{K/\rho + (K-1)\epsilon_B x} \right) e^{-x} dx P_\mu(U) \end{aligned} \quad (28)$$

where  $f(x) = e^{-x}$  is the probability density function (pdf) of  $|h|^2$ .

Next, we compute the closed-form of  $\mathbb{E}[C]$ . Based on Jensen's inequality, the expectation in (28) is upper-bounded by [31]

$$\begin{aligned} &\mathbb{E} \left[ \log_2 \left( 1 + \frac{|h|^2}{K/\rho + (K-1)\epsilon_B|h|^2} \right) \right] \\ &\leq \log_2 \left( 1 + \mathbb{E} \left[ \frac{|h|^2}{K/\rho + (K-1)\epsilon_B|h|^2} \right] \right) \\ &= \log_2 \left( 1 + \int_0^\infty \frac{x e^{-x}}{K/\rho + (K-1)\epsilon_B x} dx \right) \\ &= \log_2 \left( 1 + \frac{\gamma}{\omega^2} e^{\frac{\gamma}{\omega}} \text{Ei} \left( -\frac{\gamma}{\omega} \right) + \frac{1}{\omega} \right) \end{aligned} \quad (29)$$

where  $\gamma = K/\rho$ ,  $\omega = (K-1)\epsilon_B$ , and  $\text{Ei}(x) = -\int_{-x}^\infty e^{-r}/r dr$ .

Thus, an approximate closed-form of  $\mathbb{E}[C]$  is given by

$$\begin{aligned} \mathbb{E}[C] &= \sum_{k=1}^K \mathbb{E}[X_k] \\ &\leq K \log_2 \left( 1 + \frac{\gamma}{\omega^2} e^{\frac{\gamma}{\omega}} \text{Ei} \left( -\frac{\gamma}{\omega} \right) + \frac{1}{\omega} \right) P_\mu(U). \end{aligned} \quad (30)$$

Note that although the closed-form expression is an upper-bound, the performance difference is marginal which can be observed in Section V.

### V. SIMULATION RESULTS AND ANALYSIS

In simulations, we consider users in a sector as illustrated in Fig. 1. Thus, we have  $\Theta = (-60^\circ, 60^\circ)$ . Moreover, according to (4), the BS beams,  $\{\mathbf{v}_l\}$ , are generated as

$$\mathbf{v}_l = \mathbf{a}(\hat{\theta}_l), \quad l = 1, \dots, K \quad (31)$$

where  $\hat{\theta}_l = l\delta_\theta + \theta_{\text{offset}}$ . Here,  $\delta_\theta = \frac{120^\circ}{K}$  and  $\theta_{\text{offset}} = -60^\circ - \frac{\delta_\theta}{2}$ . In addition, we set  $\Psi = (-60^\circ, 60^\circ)$  and the signal-to-noise ratio (SNR),  $\rho$ , to 20 dB at any user.

Note that in **S2**, we have  $|\mathbf{a}^H(\theta)\mathbf{v}_l|^2 = 1$  if  $\theta \in \Theta_l$ , which is not true in general with the beams in (31). Thus, we need to modify this assumption with the results from the designed beams. If  $\theta \in \Theta_l$ , we have  $|\mathbf{a}^H(\theta)\mathbf{v}_l|^2 = G$ , where

$$\begin{aligned} G &= \frac{\max_{\theta \in \Theta_l} |\mathbf{a}^H(\theta)\mathbf{v}_l|^2 + \min_{\theta \in \Theta_l} |\mathbf{a}^H(\theta)\mathbf{v}_l|^2}{2} \\ &\leq 1. \end{aligned} \quad (32)$$

The value of  $\epsilon_B$  in (17) is the cross-correlation found from the beams in (31).

For comparison, seven different simulations<sup>1</sup> are considered as follows:

- "Analytical": simulations using (23);
- "R-analytical": simulations using (23) with the modified gain in (32);
- "Idealized analytical": simulations using (24);
- "Analytical-Ray": simulations using (28);
- "Analytical-Ray-CF": simulations using (30);
- "Realistic": simulations using opportunistic beamforming strategy with the channel coefficient in (14);
- "Realistic-Ray": simulations using opportunistic beamforming strategy within Rayleigh fading channels.

Figs. 5 and 6 show simulation results for the throughputs when  $K$  varies from 12 to 30 with  $U = 30$  and  $U = 50$ , respectively, where  $L_B = 40$  and  $L_U = 10$ . Obviously, the average throughput with  $U = 50$  is higher than that with  $U = 30$  since more multiuser gain can be exploited, which can also be illustrated through (22) and (23). Note that the performance obtained by the three analytical methods closely follows the "Realistic" curve, especially for a large number of users and moderate value of  $K$  that satisfies  $K \leq U$ .

<sup>1</sup>Note that the simplifications in Subsection II-C are not considered when running "Realistic" and "Realistic-Ray" simulations.

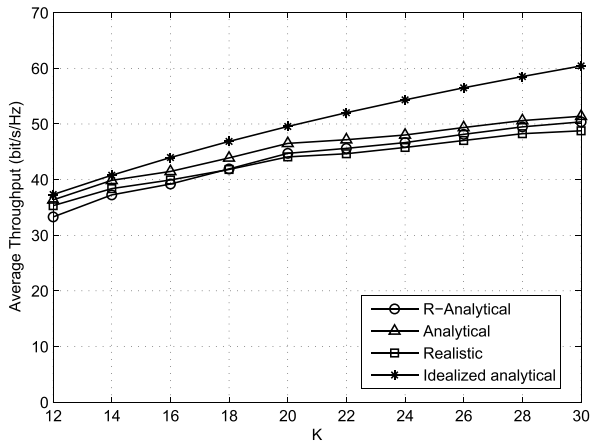


FIGURE 5. Average throughput with variable  $K$  with  $U = 30$  when  $Q = 3$  and  $N_U = 20$ .

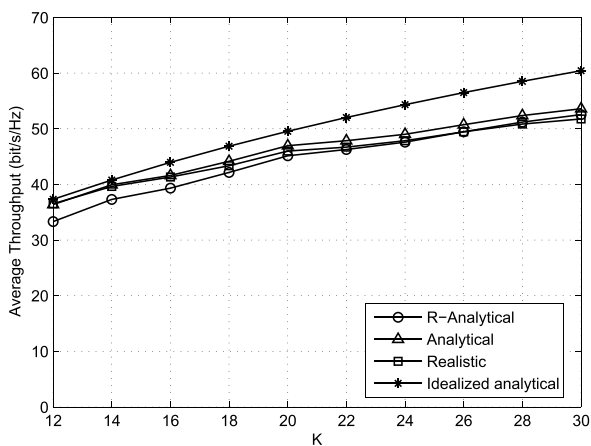


FIGURE 6. Average throughput with variable  $K$  with  $U = 50$  when  $Q = 3$  and  $N_U = 20$ .

We observe that the curve of “Analytical” is slightly higher than that of the “R-analytical” as  $G \leq 1$  from (32). In addition, “Idealized analytical” provides the highest throughput as we set  $\epsilon_B = 0.001$  which cannot be a constant in the real scenario. However, it might be a reasonable approximation with a moderate value of  $K$  and the trend agrees with that of the realistic one.

In Fig. 7, we present the simulation results for different numbers of user beams with  $U = 30$ . For “Realistic” curve, clearly, the throughput increases with  $N_U$ . Moreover, the improvement becomes less significant when  $N_U$  is sufficiently large, since the user beamforming becomes sufficiently effective. That is to say, the analytical method with the simplifications in Sections III and IV can provide a good approximation for the performance analysis if users employ a sufficiently large number of beams. Again, the throughput from “Idealized analytical” provides the highest one as we set  $\epsilon_B = 0.001$ .

When  $U = 50$ , as shown in Fig. 8, the performance gap between realistic and analytical methods becomes less significant since more multiuser gain can be exploited which results

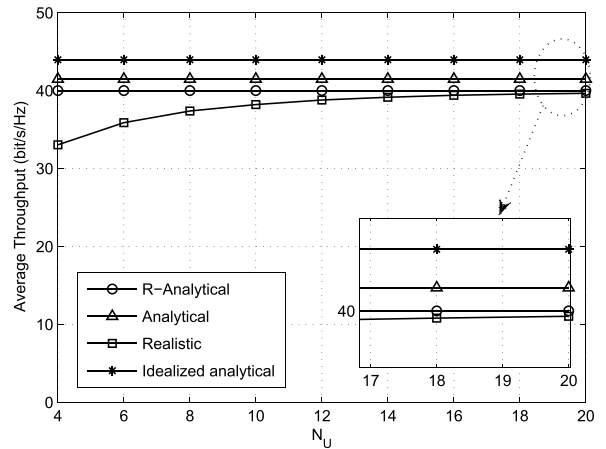


FIGURE 7. Average throughput with variable  $N_U$  when  $K = 16$ ,  $U = 30$ ,  $L_B = 40$ , and  $L_U = 10$ .

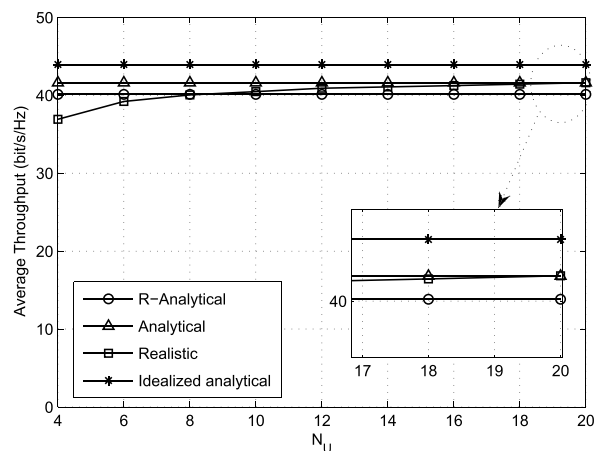


FIGURE 8. Average throughput with variable  $N_U$  when  $K = 16$ ,  $U = 50$ ,  $L_B = 40$ , and  $L_U = 10$ .

in an increasing probability of the effective beamforming among all users. In summary, the proposed analytical method can provide reasonable results when  $N_U$  is large and  $U \geq K$ .

To see the impact of  $Q$  on the effectiveness of the proposed method, simulations are carried out with  $K = 16$  and the results are shown in Fig. 9. It is noteworthy that the performance of two analytical curves closely follows that of the “Realistic” one which confirms the effectiveness of the proposed method under limited scattering environment. In addition, the further increase of  $Q$  ( $Q > 4$  in Fig. 9) does not provide a growing throughput in simulations since more IBI is involved.

For the performance with Rayleigh fading channel coefficients, the simulation results are shown in Fig. 10. Obviously, the results of analytical curves closely follow those of the numerical simulation and the average throughput grows with  $K$ . Furthermore, it can be clearly observed that there is no noticeable performance difference between “Analytical-Ray” and “Analytical-Ray-CF”, which indicates that (30) could be used as an approximate closed-form expression.

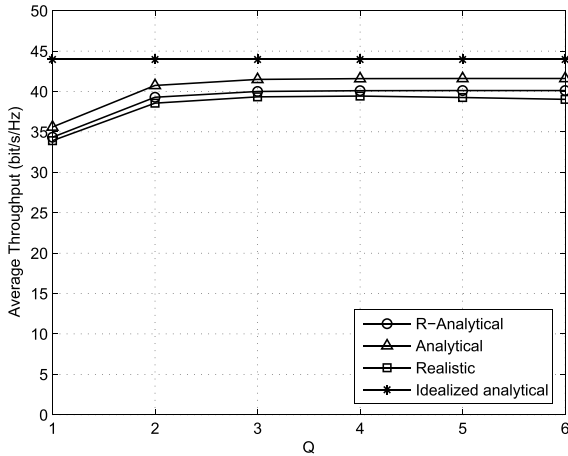


FIGURE 9. Average throughput with variable  $Q$  when  $U = 30$  and  $N_U = 12$ .

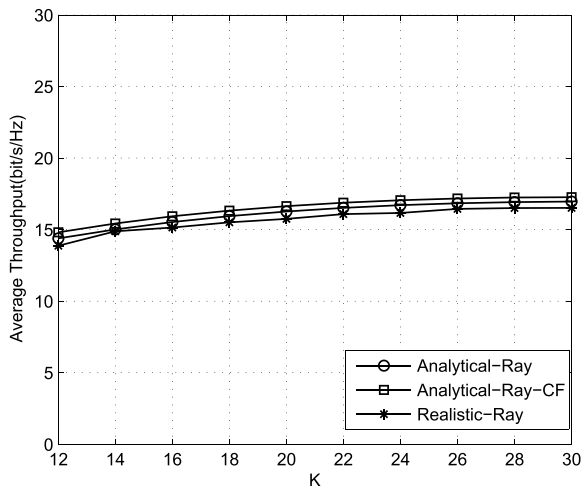


FIGURE 10. Average throughput with variable  $K$  when  $U = 30$  and  $N_U = 20$  under Rayleigh fading channels.

In addition, we can find that the impact of  $K$  on the system performance follows the discussion in Subsection IV-B.

## VI. CONCLUSION

As the mmWave channels would be characterized by much less paths than those of UHF bands, the existing approaches for performance analysis may not be useful to understand the characters in mmWave systems.

In order to analyze the downlink performance of SDMA mmWave systems with user beam selection, we proposed an approximate closed-form solution for the sum-rate where the throughput for each BS beam is formulated as a binary random variable. Moreover, unlikely the beam selection in UHF channels, when the number of users is more than that of the BS beams, we demonstrated that the downlink throughput increases with more angular resolution at the BS. It was shown that the throughput obtained from the proposed analytical method agrees with that from simulations, which confirms the effectiveness of the proposed analysis method in SDMA mmWave systems.

## REFERENCES

- [1] W. Roh et al., "Millimeter-wave beamforming as an enabling technology for 5G cellular communications: Theoretical feasibility and prototype results," *IEEE Commun. Mag.*, vol. 52, no. 2, pp. 106–113, Feb. 2014.
- [2] M. R. Akdeniz, Y. Liu, S. Rangan, and E. Erkip, "Millimeter wave picocellular system evaluation for urban deployments," in *Proc. IEEE Globecom Workshops*, Dec. 2013, pp. 105–110.
- [3] Y. Roy, J.-Y. Chouinard, and S. A. Mahmoud, "Selection diversity combining with multiple antennas for mm-wave indoor wireless channels," *IEEE J. Sel. Areas Commun.*, vol. 14, no. 4, pp. 674–682, May 1996.
- [4] S. Sun, T. S. Rappaport, R. W. Heath, Jr., A. Nix, and S. Rangan, "MIMO for millimeter-wave wireless communications: Beamforming, spatial multiplexing, or both?" *IEEE Commun. Mag.*, vol. 52, no. 12, pp. 110–121, Dec. 2014.
- [5] T. S. Rappaport et al., "Millimeter wave mobile communications for 5G cellular: It will work!" *IEEE Access*, vol. 1, pp. 335–349, May 2013.
- [6] T. Bai, R. Vaze, and R. W. Heath, Jr., "Analysis of blockage effects on urban cellular networks," *IEEE Trans. Wireless Commun.*, vol. 13, no. 9, pp. 5070–5083, Sep. 2014.
- [7] T. Bai and R. W. Heath, Jr., "Coverage and rate analysis for millimeter-wave cellular networks," *IEEE Trans. Wireless Commun.*, vol. 14, no. 2, pp. 1100–1114, Feb. 2015.
- [8] A. Gupta and R. K. Jha, "A survey of 5G network: Architecture and emerging technologies," *IEEE Access*, vol. 3, pp. 1206–1232, Jul. 2015.
- [9] M. K. Samimi et al., "28 GHz angle of arrival and angle of departure analysis for outdoor cellular communications using steerable beam antennas in New York City," in *Proc. IEEE VTC Spring*, Jun. 2013, pp. 1–6.
- [10] H. Zhang, S. Venkateswaran, and U. Madhow, "Channel modeling and MIMO capacity for outdoor millimeter wave links," in *Proc. IEEE WCNC*, Apr. 2010, pp. 1–6.
- [11] O. El Ayach, S. Rajagopal, S. Abu-Surra, Z. Pi, and R. W. Heath, Jr., "Spatially sparse precoding in millimeter wave MIMO systems," *IEEE Trans. Wireless Commun.*, vol. 13, no. 3, pp. 1499–1513, Mar. 2014.
- [12] W. Choi, A. Forenza, J. G. Andrews, and R. W. Heath, Jr., "Opportunistic space-division multiple access with beam selection," *IEEE Trans. Commun.*, vol. 55, no. 12, pp. 2371–2380, Dec. 2007.
- [13] C. W. Tan, M. Chiang, and R. Srikant, "Maximizing sum rate and minimizing MSE on multiuser downlink: Optimality, fast algorithms and equivalence via max-min SINR," *IEEE Trans. Signal Process.*, vol. 59, no. 12, pp. 6127–6143, Dec. 2011.
- [14] M. Schubert and H. Boche, "Solution of the multiuser downlink beamforming problem with individual SINR constraints," *IEEE Trans. Veh. Technol.*, vol. 53, no. 1, pp. 18–28, Jan. 2004.
- [15] S.-R. Lee, H.-B. Kong, H. Park, and I. Lee, "A new beamforming design based on random matrix theory for weighted sum-rate maximization in interference channels," in *Proc. IEEE Globecom Conf.*, Dec. 2013, pp. 3614–3619.
- [16] X. Meng, X. G. Gao, and X.-G. Xia, "Omnidirectional precoding based transmission in massive MIMO systems," *IEEE Trans. Commun.*, vol. 64, no. 1, pp. 174–186, Jan. 2016.
- [17] G. Bartoli et al., "Beamforming for small cell deployment in LTE-advanced and beyond," *IEEE Wireless Commun.*, vol. 21, no. 2, pp. 50–56, Apr. 2014.
- [18] W. Yu and J. M. Cioffi, "Sum capacity of Gaussian vector broadcast channels," *IEEE Trans. Inf. Theory*, vol. 50, no. 9, pp. 1875–1892, Sep. 2004.
- [19] C. Xing, N. Wang, J. Ni, Z. Fei, and J. Kuang, "MIMO beamforming designs with partial CSI under energy harvesting constraints," *IEEE Signal Process. Lett.*, vol. 20, no. 4, pp. 363–366, Apr. 2013.
- [20] M. Sharif and B. Hassibi, "On the capacity of MIMO broadcast channels with partial side information," *IEEE Trans. Inf. Theory*, vol. 51, no. 2, pp. 506–522, Feb. 2005.
- [21] Z. Xiao, L. Bai, and J. Choi, "Iterative joint beamforming training with constant-amplitude phased arrays in millimeter-wave communications," *IEEE Commun. Lett.*, vol. 18, no. 5, pp. 829–832, May 2014.
- [22] A. Abbaspour-Tamijani and K. Sarabandi, "An affordable millimeter-wave beam-steerable antenna using interleaved planar subarrays," *IEEE Trans. Antennas Propag.*, vol. 51, no. 9, pp. 2193–2202, Sep. 2003.
- [23] J. A. Zhang, X. Huang, V. Dyadyuk, and Y. J. Guo, "Massive hybrid antenna array for millimeter-wave cellular communications," *IEEE Wireless Commun.*, vol. 22, no. 1, pp. 79–87, Feb. 2015.
- [24] R. Méndez-Rial, C. Rusu, N. González-Prelcic, A. Alkhateeb, and R. W. Heath, Jr., "Hybrid MIMO architectures for millimeter wave communications: Phase shifters or switches?" *IEEE Access*, vol. 4, pp. 247–267, Jan. 2016.



- [25] R. Rajashekar and L. Hanzo, "Hybrid beamforming in mm-wave MIMO systems having a finite input alphabet," *IEEE Trans. Commun.*, vol. 64, no. 8, pp. 3337–3349, Aug. 2016.
- [26] J. Kang, I.-K. Choi, D.-S. Kwon, and C. Lee, "An opportunistic beamforming technique using a quantized codebook," in *Proc. IEEE VTC Spring*, Apr. 2007, pp. 1647–1651.
- [27] K. Ramachandran, R. Kokku, R. Mahindra, and K. Maruhashi, "On the potential of fixed-beam 60 GHz network interfaces in mobile devices," in *Proc. PAM*, Mar. 2011, pp. 62–71.
- [28] D. Liu and Y. P. Zhang, "Integration of array antennas in chip package for 60-GHz radios," *Proc. IEEE*, vol. 100, no. 7, pp. 2364–2371, Jul. 2017.
- [29] J. Choi, "Beam selection in mm-wave multiuser MIMO systems using compressive sensing," *IEEE Trans. Commun.*, vol. 63, no. 8, pp. 2936–2947, Aug. 2015.
- [30] J. Choi, "On the performance of multiuser beam selection at base station and user arrays in mm-wave systems," in *Proc. ICUFN*, Jul. 2015, pp. 929–934.
- [31] I. S. Gradshteyn and I. M. Ryzhik, *Table of Integrals, Series and Products*, 7th ed. New York, NY, USA: Academic, 2007.



**LIN BAI** (M'13–SM'17) received the B.Sc. degree in electronics and information engineering from the Huazhong University of Science and Technology, Wuhan, China, in 2004, the M.Sc. degree (Hons.) in communication systems from the University of Wales, Swansea, U.K., in 2007, and the Ph.D. degree in advanced telecommunications from the School of Engineering, Swansea University, U.K., in 2010. He has been with the School of Electronics and Information Engineering, Beihang University, Beijing, China, as an Associate Professor since 2011. He has authored the books *Low Complexity MIMO Detection* (Springer, 2012) and *Low Complexity MIMO Receivers* (Springer, 2014).

His research interests include signal processing of wireless communications, particularly multiple-input multiple-output systems, array/smart antenna, and lattice-based approaches. He received an IEEE COMMUNICATIONS LETTERS Exemplary Reviewers Certificate for 2012 and the Best Paper Award from ICNS 2013 (Conference). He also served as a Guest Editor of the *International Journal of Distributed Sensor Networks* from 2012 to 2014. He is currently an Editor of the *KSII Transactions on Internet and Information Systems* and a Managing Editor of the *Journal of Communications and Information Networks*.



**TIAN LI** (S'17) received the B.E. degree from Hebei University, Baoding, China, in 2010, and the M.E. degree in control science and engineering from the Beijing Institute of Technology, Beijing, China, in 2013. He is currently pursuing Ph.D. degree in information and communication engineering with the School of Electronic and Information Engineering, Beihang University, Beijing. His current research interests include areas of wireless communications, including multiple-input

multiple-output detections and millimeter-wave systems.



**ZHENYU XIAO** (M'11–SM'17) received the B.E. degree with the Department of Electronics and Information Engineering, Huazhong University of Science and Technology, Wuhan, China, in 2006, and the Ph.D. degree with the Department of Electronic Engineering, Tsinghua University, Beijing, China, in 2011. From 2011 to 2013, he held a post-doctoral position with the Electronic Engineering Department, Tsinghua University. From 2013 to 2016, he was a Lecturer with the Department of

Electronic and Information Engineering, Beihang University, Beijing, where he is currently an Associate Professor.

He has published over 60 papers. He is currently dedicated in millimeter-wave communications and UAV communication networks. His research interests are communication signal processing and practical system implementation for wideband communication systems. He has been a TPC Member of the IEEE GLOBECOM'12, the IEEE WCSP'12, and the IEEE ICC'15. He served as a Reviewer of the IEEE TRANSACTIONS ON SIGNAL PROCESSING, the IEEE TRANSACTIONS ON WIRELESS COMMUNICATIONS, the IEEE TRANSACTIONS ON VEHICULAR TECHNOLOGY, and the IEEE COMMUNICATIONS LETTERS. He is currently an Editor of the IEEE ACCESS.



**JINHO CHOI** (M'91–SM'02) was born in Seoul, South Korea. He received the B.E. (*magna cum laude*) degree in electronics engineering from Sogang University, Seoul, in 1989, and the M.S.E. and Ph.D. degrees in electrical engineering from the Korea Advanced Institute of Science and Technology, Daejeon, in 1991 and 1994, respectively. He was with the College of Engineering, Swansea University, U.K., as a Professor/Chair in wireless.

In 2013, he joined the Gwangju Institute of Science and Technology, where he is currently a Professor. He authored two books published by Cambridge University Press in 2006 and 2010. His research interests include wireless communications and array/statistical signal processing. He received the 1999 Best Paper Award for Signal Processing from EURASIP and the 2009 Best Paper Award from WPMC (Conference). He served as an Associate Editor or Editor of other journals, including the IEEE COMMUNICATIONS LETTERS, the *Journal of Communications and Networks*, the IEEE TRANSACTIONS ON VEHICULAR TECHNOLOGY, and the *ETRI Journal*. He is currently an Editor of the IEEE TRANSACTIONS ON COMMUNICATIONS.

• • •